An Integrated Multi-beam Optical Beamformer Architecture with Beam-Shaping Capabilities.

Stefanos Kovaios[(1),(2)], Ioannis Roumpos[(1),(2)], Ronis Maximidis[(1),(2)] , Anna Timiani[(2),(3)], Apostolos Tsakyridis[(1),(2)], George Giamougiannis[(1),(2)], Miltiadis Moralis-Pegios[(1),(2)], Nikos Pleros [(1),(2)]

[(1)] School of Informatics, Aristotle University of Thessaloniki, 54124, Thessaloniki, Greece
sdkovaios@csd.auth.gr
[(2)] Center of Interdisciplinary Research & Innovation, Balkan Center, 57001, Thessaloniki, Greece
[(3)] School of Electrical and Computer Engineering, Aristotle University of Thessaloniki, 54124, Thessaloniki, Greece

Abstract *Recent demonstrations of optical phased arrays lack the capability of generating simultaneously multiple beams. We propose an optical multibeam beamformer with independent beams control, relying on a crossbar architecture. The beamforming was validated experimentally, with achieved steering angles up to 8° and two-beam generation.*

Introduction

Beamsteering and beamforming networks comprise critical functions in both the radiofrequency (RF) and free-space optics (FSO) application areas, allowing higher wireless communication speeds and higher scanning resolution metrics in the 5G/6G communication and sensing application segments respectively.

With the rapid penetration of Photonic Integrated Circuit (PIC) technologies into both the RF and FSO system area, beamformer circuits seem to greatly benefit from the reduced size, energy and cost credentials of PIC technology. So far, PIC-based optical beamformers have demonstrated some highly reliable alternatives compared to the bulky and energy-hungry RF chains and mechanical steering systems [1]–[4] employed in respective RF and FSO systems. The successful transfer of Phased Antenna Array (PAA) concepts into the FSO segment has introduced the Optical Phased Array (OPA) technology [5]–[7] with a highly directive beam generated by utilizing a large number of tightly spaced optical antennas, each connected to a phase-modulating (PM) element. An OPA generates a single steerable beam (Fig. 1(a)), while in practical applications multibeam capabilities are required. The generation of multiple beams can be achieved by the simultaneous use of several PAA configurations, each generating a single beam (Fig.1(b)). However this approach inevitably increases the number of radiating elements by a factor equal to the number of the desired beams, and consequently the overall PIC footprint. Considering, for example, the recently demonstrated 8192 element array of 5 mm long optical radiators with (8×5) mm^2 aperture [8], its scaling to N parallel beams would lead to (N× 8×5) mm^2 footprint that would comprise almost

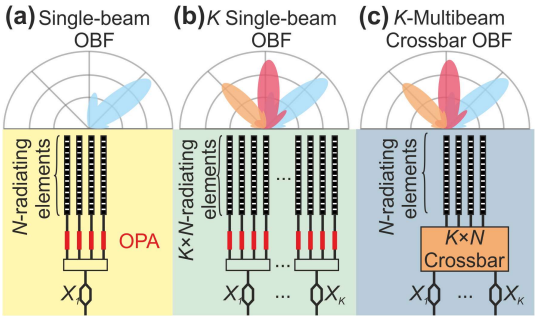

Fig. 1: Optical beamforming techniques. a) Single beam OBF, requiring N radiating elements. b) Multibeaming realized with *K* single OBFs, requiring *K*×*N* radiating elements. c) Multibeaming realized with *K*×*N* Xbar, requiring *N* radiating elements

20% of the silicon die area when N=2 and close to 40% when N increases to 4.

This issue was resolved in the microwave domain by adopting multibeam beamforming network architectures, allowing the use of the same radiating elements for the generation of all N beams [9]. However, Optical Multi-beam beamformer network (OMBFN) architectures have been demonstrated mostly in simulations [10]–[16]. On top of that, they rely mainly on complex unitary optical linear Mach-Zehnder Interferometer meshes, resulting to strong interdependencies between the PMs, so that every beam cannot be generated and steered independently.

In this paper, we propose the deployment of the crossbar (Xbar)-based universal linear operator [17] as an OMBFN, allowing the independent generation and control of multiple simultaneous beams (Fig.1(c)). The experimental demonstration of the Xbar-based OMBFN, was performed on a SiPho 4×4 Xbar chip, revealing a 25 mW pi-shift per phase shifter. Finally, we validate the Xbar beam shaping capabilities by

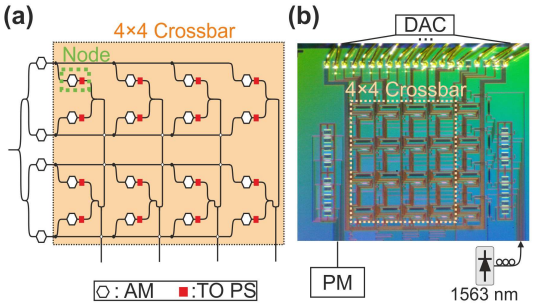

Fig. 2: a) The 4×4 Xbar layout. b) The experimental setup used for the optical characterization of the 4×4 Xbar.

predicting the generation of two independent beams, with achievable steering angles up to 8° and side lobe level down to -16 dB.

Operation principles and experimental setup

The layout of the 4×4p Xbar deployed for the OMBFN's experimental validation is presented in Fig. 2(a). The 4×4 Xbar is constructed by interconnecting optical computation nodes. Each computation node consists of an amplitude modulator (AM) and a PM, aggregately allowing the amplitude and phase control of the different optical signals. This architecture allows natural one-to-one mapping of each matrix element into the designated Xbar node, avoiding cascaded nodes which leads to the lowest loss linear optical architecture [17] with independent amplitude and phase control translating to multiple independent beam generation and robustness to fabrication errors setting the optical crossbar as a favorable optical multibeam beamformer network (OMBFN).

The experimental validation of the Xbar beamforming capabilities was explored on a 4×4 SiPho Xbar chip fabricated in imec's ISSIPP50G platform [18], initially designed for high-rate neuromorphic optical processing applications. The fabricated crossbar, presented in Fig. 2(b) consists of 16 computational nodes, each encompassing a SiGe electro-absorption modulator (EAM) and a thermo-optical (TO) PM. The photonic chip is attached to a printed circuit board (PCB) and the stable electrical control of the PIC components is performed through an external electrical digital-to-analog converter (DAC) through multiple wire bondings. The optical measurements are performed with a continuous wave (CW) optical signal, generated by a tunable laser, with a wavelength of 1563 nm, matching the optimal response of the stand-alone EAMs. The optical outputs are captured by an optical power meter. The optical fiber-to-fiber losses have been identified to approximately 8 dB, which can be deduced to 5 dB loss of the grating couplers and 3 dB of coupling loss.

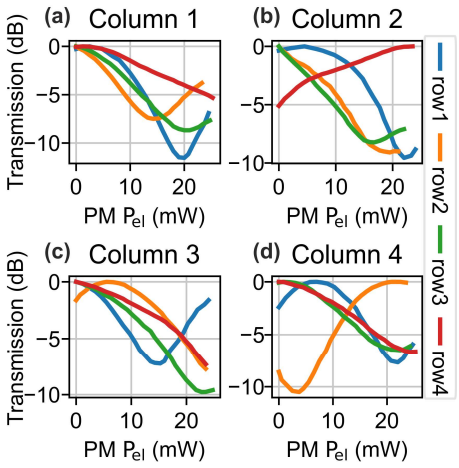

Fig. 3: Measured transmission under variation of the PM as a function of the individual PM's power consumption, indicating that pi-shift can be achieved at approximately 20 mW

Experimental results

Firstly, the characterization of the Xbar's nodes is performed. In Fig. 3, the measured optical output power of the Xbar is recorded under the variation of each node's PM independently, in a voltage range corresponding to an electrical applied power of 0 – 25 mW. It is clear from the presented results that most phase shifters exhibit pi-phase shifts in the defined power range, except for the PMs of row 4, due to the degraded electrical on-chip connections. The AMs of the Xbar's nodes exhibit a 4.5 dB extinction ratio (ER), as described in [18].

Following the optical characterization of the Xbar, we proceed with the validation of the Xbar's OMBFN capabilities. Since the direct evaluation of the Xbar's beamforming is not feasible due to the absence of radiators, we perform an indirect procedure relying on a series of optical power measurements, with the optical signal being fed to the 4 ports of the crossbar. In these measurements, 3 PMs of each row are varied simultaneously, in a reduced electrical power range of 0 - 10 mW, to minimize the effect of thermal crosstalk. Based on these measurements, a theoretical model of the Xbar was deployed, accounting for optical amplitude variations and moderate crosstalk effects, in order to obtain the phase shifts induced by each PM. The experimental and theoretical results are presented in Fig. 4 (a), with an evaluated mean squared error (MSE) below 0.01 for all cases, confirming the validity of the proposed model.

To achieve steering of the generated beams, the optical radiators need to be fed with optical fields featuring specific relative phase differences. From the available measurements, we isolate subsets with phase differences,

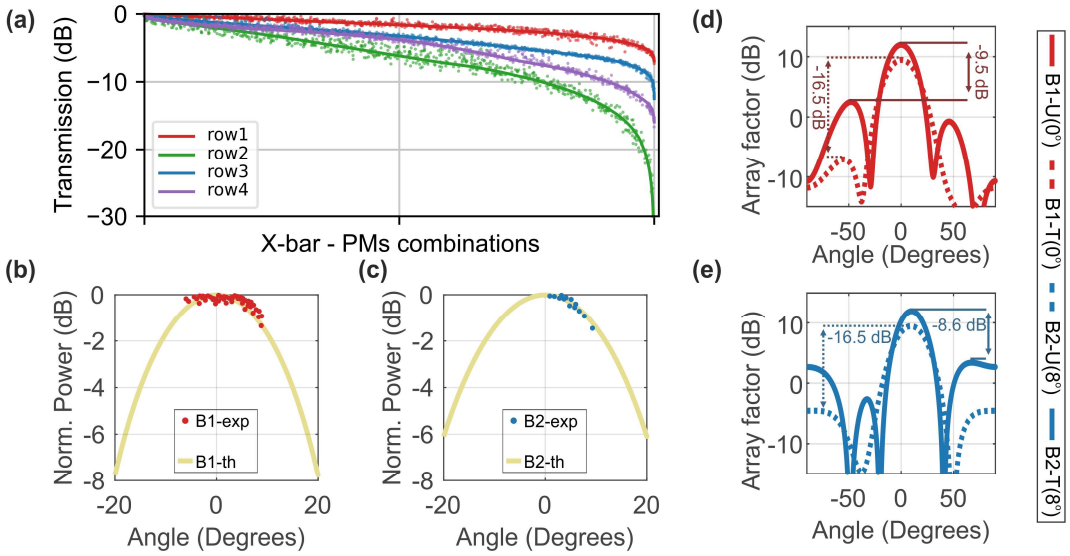

Fig. 4: OMBFN 4×4 crossbar. a) Experimental and theoretical optical outputs for different combinations of 3 PMs, depicting the validity of our models. b)-c) Observed and predicted optical power of as a function of the achievable steering angle for two Xbar beams B1, B2. e) Predicted radiation patterns of the two independent beams B1, B2.

leading to construction of beams towards characteristic steering angles and optical output power of the Xbar. Figs. 4(b)-(c) show the experimentally obtained and theoretically calculated Xbar optical power corresponding to the identified steering angles, for two generated beams B1 (row 1) and B2 (row 3) respectively, validating the multibeam operation of the device. The steering angles were evaluated under the assumption that the Xbar's optical output is directed to an array of 4 isotropic radiators with a pitch of 700 nm. The deviation of the experimental results from the theoretical curve is due to the coarse measurement set, originating from the necessity of tuning three PMs simultaneously.

Finally, the corresponding radiation patterns for experimentally obtained PM settings for two different uniformly fed beams (B1-U and B2-U) at 0° and 8° are presented in Fig. 4(d)-(e) respectively. To validate the beamshaping capabilities of the OMBFN, we introduce 3 dB loss to the AMs of the edge elements, which leads to 7 dB and 8 dB reduction in side lobe level for beam B1 (B1-T) and beam B2 (B2-T) respectively.

Conclusions

In this paper, we proposed the novel OMBFN Xbar-based architecture, enabling the independent generation and control of multiple beams. The experimental characterization of the 4×4 Xbar revealed a 25 mW pi-shift per phase shifter. The validity of the expected Xbar OMBFN operation was established through an indirect experimental and theoretical study. The multiple beam generation was confirmed through the generation of phase settings in row 1 and row 2 of the Xbar, which corresponded to two independent beams, steered at 0° and 8° respectively. Finally, the beam shaping potential through side lobe suppression, by approximately 7.5 dB, was achieved by tuning particular AMs for and tapering the Xbar optical output.

The performance of the proposed Xbar OMBFN can be significantly improved by implementing the proposed scheme with phase shifters that would encompass greater tuning range and reduced coupling, such as electro-optical or piezo-electric phase modulators. Finally, the replacement of the EAMs with AMs encompassing greater ER values and improved thermal stability would further enhance the overall OMBFN beamshaping prospect of the Xbar architecture.

Acknowledgements

This work was supported by the EU through the HORIZON project PARALIA (PN: 101093013) and the HORIZON Marie-Curie PF project MIMOSA (PN: 101065845). The authors would like to acknowledge Keysight for supporting the experiments with measurement equipment.

References

[1] A. Harris, J. J. S. Jr., H. H. Refai, and P. G. LoPresti, “Comparison of active beam steering elements and analysis of platform vibrations for various long-range FSO links,” in *Digital Wireless Communications VII and Space Communication Technologies*, 2005, vol. 5819, pp. 474–484, doi: 10.1117/12.603667.

[2] P. Deng, M. Kavehrad, and Y. Lou, “MEMS-based beam-steerable FSO communications for reconfigurable wireless data center,” in *Broadband Access Communication Technologies XI*, 2017, vol. 10128, p. 1012805, doi: 10.1117/12.2253342.

[3] R. Halterman and M. Bruch, “Velodyne HDL-64E lidar for unmanned surface vehicle obstacle detection,” in *Unmanned Systems Technology XII*, 2010, vol. 7692, p. 76920D, doi: 10.1117/12.850611.

[4] D. Wang, C. Watkins, and H. Xie, “MEMS Mirrors for LiDAR: A Review,” *Micromachines*, vol. 11, no. 5, 2020, doi: 10.3390/mi11050456.

[5] Y. Guo, Y. Guo, C. Li, H. Zhang, X. Zhou, and L. Zhang, “Integrated Optical Phased Arrays for Beam Forming and Steering,” *Applied Sciences*, vol. 11, no. 9, 2021, doi: 10.3390/app11094017.

[6] C.-P. Hsu *et al.*, “A Review and Perspective on Optical Phased Array for Automotive LiDAR,” *IEEE Journal of Selected Topics in Quantum Electronics*, vol. 27, no. 1, pp. 1–16, 2021, doi: 10.1109/JSTQE.2020.3022948.

[7] H. Hashemi, “A Review of Semiconductor-Based Monolithic Optical Phased Array Architectures,” *IEEE Open Journal of the Solid-State Circuits Society*, vol. 1, pp. 222–234, 2021, doi: 10.1109/OJSSCS.2021.3120238.

[8] C. V Poulton, M. J. Byrd, B. Moss, E. Timurdogan, R. Millman, and M. R. Watts, “8192-Element Optical Phased Array with 100° Steering Range and Flip-Chip CMOS,” in *2020 Conference on Lasers and Electro-Optics (CLEO)*, 2020, pp. 1–2.

[9] Y. J. Guo, M. Ansari, and N. J. G. Fonseca, “Circuit Type Multiple Beamforming Networks for Antenna Arrays in 5G and 6G Terrestrial and Non-Terrestrial Networks,” *IEEE Journal of Microwaves*, vol. 1, no. 3, pp. 704–722, 2021, doi: 10.1109/JMW.2021.3072873.

[10] W. Charczenko, M. R. Surette, P. J. Matthews, H. Klotz, and A. R. Mickelson, “Integrated optical Butler matrix for beam forming in phased-array antennas,” in *Optoelectronic Signal Processing for Phased-Array Antennas II*, 1990, vol. 1217, pp. 196–206, doi: 10.1117/12.18158.

[11] J. T. Gallo and R. DeSalvo, “Experimental demonstration of optical guided-wave Butler matrices,” *IEEE Transactions on Microwave Theory and Techniques*, vol. 45, no. 8, pp. 1501–1507, 1997, doi: 10.1109/22.618463.

[12] B. Li, Y. Chen, N. Jiang, Z. Fu, S. Tang, and R. T. Chen, “Photonic phased-array antenna system based on detector-switched optical Blass matrix true-time-delay steering and heterodyne rf generation,” in *Applications of Photonic Technology 4*, 2000, vol. 4087, pp. 1004–1007, doi: 10.1117/12.406340.

[13] D. Madrid, B. Vidal, A. Martinez, V. Polo, J. L. Corral, and J. Marti, “A novel 2N beams heterodyne optical beamforming architecture based on N/spl times/N optical Butler matrices,” in *2002 IEEE MTT-S International Microwave Symposium Digest (Cat. No.02CH37278)*, 2002, vol. 3, pp. 1945–1948 vol.3, doi: 10.1109/MWSYM.2002.1012245.

[14] J. Guo, M. Li, P. Chen, H. Zhang, and X. Yu, “A Multi-Beam Network Based on Silicon-Based Optical Waveguide,” in *2018 11th UK-Europe-China Workshop on Millimeter Waves and Terahertz Technologies (UCMMT)*, 2018, vol. 1, pp. 1–3, doi: 10.1109/UCMMT45316.2018.9015747.

[15] C. Tsokos *et al.*, “Analysis of a Multibeam Optical Beamforming Network Based on Blass Matrix Architecture,” *Journal of Lightwave Technology*, vol. 36, no. 16, pp. 3354–3372, 2018, doi: 10.1109/JLT.2018.2841861.

[16] P. M.-C. Romero *et al.*, “Integrated Microwave Photonics Coherent Processor for Massive-MIMO Systems in Wireless Communications,” *IEEE Journal of Selected Topics in Quantum Electronics*, vol. 29, no. 6: Photonic Signal Processing, pp. 1–12, 2023, doi: 10.1109/JSTQE.2023.3264434.

[17] G. Giamougiannis *et al.*, “A Coherent Photonic Crossbar for Scalable Universal Linear Optics,” *Journal of Lightwave Technology*, vol. 41, no. 8, pp. 2425–2442, 2023, doi: 10.1109/JLT.2023.3234689.

[18] G. Giamougiannis, M. Moralis-Pegios, A. Tsakyridis, N. Bamiedakis, D. Lazovsky, and N. Pleros, “On-Chip Universal Linear Optics using a 4x4 Silicon Photonic Coherent Crossbar,” in *Optical Fiber Communication Conference (OFC) 2023*, 2023, p. Tu3B.3, [Online]. Available: https://opg.optica.org/abstract.cfm?URI=OFC-2023-Tu3B.3.